RESEARCH

Effect of Extrusion on the Functional, Textural and Colour Characteristics of Texturized Hempseed Protein

Amrut Rajendra[1] · Danyang Ying[2] · Robyn Dorothy Warner[1] · Minh Ha[1] · Zhongxiang Fang[1]

Abstract

The search for allergy friendly texturized vegetable proteins (TVP) has prompted the use of novel protein sources over conventional wheat and soy proteins. Hempseed protein (HP) offers promising nutritional characteristics. This work assessed the effect of feed moisture content (FMC) and screw rotation speed (SRS) on the textural, functional and colour characteristics of texturized HP. The HP was extruded using a co-rotation twin screw extruder at 30–60% FMC and 200–400 rpm SRS. Results showed that significant differences were observed from FMC, SRS and the interaction of FMC and SRS on the product expansion index, integrity index, water and oil absorption capacity (WAC and OAC), some texture profile parameters and colour characteristics. Decreasing FMC and increasing SRS tended to increase the texturization index, expansion index, WAC, OAC, integrity index and texture profile characteristics but decrease density, $L*$ and $b*$ values. These results contribute to our understanding of the properties of texturized HP which are important for application in food industry.

Keywords Extrusion · Hempseed protein · Texturized vegetable protein · Feed moisture content · Screw rotation speed

Abbreviations
FMC   Feed moisture content
HP   Hempseed protein
OAC   Oil absorption capacity
SRS   Screw rotation speed
THC   Tetrahydrocannabinol
TVP   Texturized vegetable protein
WAC   Water absorption capacity

Introduction

With the world population expected to reach 9.7 billion by 2050, there is a great need for sustainable, palatable and affordable protein sources (Sun et al., 2020). The production of animal proteins consumes significant resources at a considerable cost to the environment due to high greenhouse gas emissions, deforestation, water consumption, biodiversity loss and nutrient leaching (Godfray et al., 2018).

✉ Zhongxiang Fang
  Zhongxiang.fang@unimelb.edu.au

1 Faculty of Veterinary and Agricultural Sciences, The University of Melbourne, Parkville, VIC 3010, Australia

2 CSIRO Agriculture & Food, 671 Sneydes Road, Werribee, Vic 3030, Australia

Furthermore, diets high in processed and red meats are associated with increased risk of cardiovascular disease, type 2 diabetes and certain types of cancer (Richi et al., 2015). Such environmental as well as health, ethical, food security and convenience factors have promoted the demand for meat analogues, with the Australian meat analogue market expected to be valued at $3 billion by 2030 (Curtain & Grafenauer, 2019; Dekkers et al., 2018; Lawrence & King, 2019). Texturized vegetable protein (TVP) is defined as an edible food product produced through extrusion of plant proteins and is often a key ingredient in meat analogues (Riaz, 2011). Currently, TVP is predominantly produced from defatted soy and wheat gluten sources (De Angelis et al., 2020). However, alternative protein sources are needed because the current dominant soy and wheat protein products are not allergen friendly, with further concerns regarding unsustainable production and genetic modification of soy (Thrane et al., 2017; Webb et al., 2020). While protein sources other than wheat and soy have been assessed on their ability to form TVP, few are texturally adequate and economically viable and have sufficient supply of raw materials (Riaz, 2011).

Hempseed protein concentrate (HPC) is produced from hempseed cake which is a by-product of hempseed oil extraction. It boasts a strong nutritional profile as it contains all essential amino acids with good protein digestibility (Pihlanto et al., 2020). Unlike soy and wheat sources, HPC

does not contain common allergens which presents labelling advantages and novelty over conventional products (Webb et al., 2020). Despite these benefits, there is currently limited research on hempseed protein.

Extrusion is essential to produce TVP and is the most common commercial technique to transform plant protein materials into fibrous products (Dekkers et al., 2018). During extrusion, protein molecules undergo conformational changes including hydration, heating, denaturation, alignment, collision and aggregation via covalent and noncovalent cross-linking which produces the characteristic textures of TVP (Beniwal et al., 2021). Extrusion parameters including screw rotation speed (SRS) and feed moisture content (FMC) can alter final product characteristics including textural, nutritional, sensory and functional characteristics (Zhang et al., 2019). FMC acts as a plasticizer and lubricant, participates in reactions, determines the viscosity and ensures dough melting, while also influencing other system parameters (Chen et al., 2010; Plattner, 2020). Contrastingly, SRS is necessary as it provides shear force and viscous dissipation to enable temperature distribution and sufficient mixing while conveying the melt through the extruder (Zhang et al., 2019). In soy, wheat and other proteins, authors have noted that modifying FMC impacts density, expansion, porosity, fibre formation, tensile strength, chewiness, hardness and integrity while SRS has been identified to modify texturization (Chen et al., 2010; Fang et al., 2014; Palanisamy et al., 2019). While there is an abundance of research on the effect of extrusion parameters on soy and wheat protein sources, there is no research evaluating the effect of extrusion parameters on HPC. Thus, this research investigates how the FMC and SRS impact on extruded HPC's functional, colour and textural characteristics. This research would provide a practical reference for the industrial production of TVP from HPC.

Materials and Methods

Materials and Sample Preparation

Hempseed protein concentrate (HPC) was kindly supplied by Australian Primary Hemp (Melbourne, Australia) and was vacuum packaged in vacuum sealer bags made of polyamide (PA) and polyethylene (PE). The nutritional content of HPC was characterized by about 51.71% protein (Kjeldahl method, conversion factor of 6.25), 13.80% lipid (Soxhlet extraction) and 25.43% carbohydrates (phenol sulphuric acid method) with moisture content at 9.58% (gravimetric method). Deionized water was acquired from Millipore Milli-Q gradient water purification system (Darmstadt, HE, Germany). All chemicals were purchased from Sigma-Aldrich Co. (North Ryde, NSW, Australia) unless otherwise stated.

Extrusion of Products

Pre-trials were initially conducted to determine the FMC, SRS and barrel temperature ranges which could produce an extrudable product. HPC was extruded using a KDT30-II co-rotating twin screw extruder (Jinan Kredit Machinery Co Ltd., Shandong, China) with a screw diameter of 20 mm, screw length/diameter ratio of 20:1 and a fixed screw configuration (Fig. 1). The extruder had four different temperature zones in the barrel and suitable temperatures were determined at 50 °C, 80 °C, 120 °C and 80 °C respectively as they produced a consistently extruded product. These temperatures were maintained throughout the extrusion process by an electric cartridge heating system and a running watercooling system. The FMC was adjusted with a FEDOS E8 piston water dosing pump (Lutz-Jesco, NI, Germany). The target FMC was calculated using the moisture content of raw materials and was maintained by adjusting solid dosing (0.8–1.1 kg/h) and liquid dosing (1.88–2.36 kg/h). The mixture was pushed through a 25-mm circular cooling die and cooling die outlet maintained at 59 °C. From the pretrials, FMC and SRS extrusion parameters were chosen by selecting the widest range within this working window. Thus, a complete experimental design with four FMC (30%, 40%, 50% and 60%) and three SRS (200 rpm, 300 rpm and 400 rpm) was selected as listed in Table 1.

Duplicate trials of these conditions were subsequently tested. Once parameters were modified, 15 min was allowed for parameters to stabilize, and samples were subsequently collected for 5 min. The extrudate was manually cut at the end of the cooling die and cooled at room temperature. The material was vacuum sealed in in the vacuum sealer bags and stored at refrigeration temperature below 4 °C until
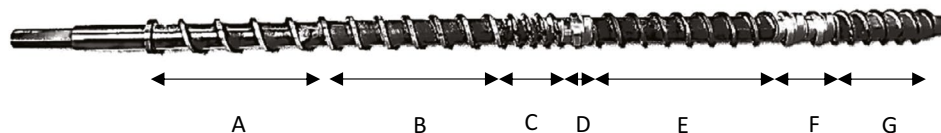

Fig. 1 Configuration of screw components used for extrusion processing. Letters reference different screw components: **A**, full pitch screw; **B**, 2/3 pitch screw; **C**, 1/4 pitch screw; **D**, reverse kneading block; **E**, 2/3 pitch screw; **F**, reverse kneading block; **G**, 1/2 pitch screw

Table 1 Feed moisture and screw rotation speed conditions tested for extrusion of hempseed protein concentrate

Condition	Feed moisture content (%)	Screw rotation speed (rpm)
F60S200	60	200
F60S300	60	300
F60S400	60	400
F50S200	50	200
F50S300	50	300
F50S400	50	400
F40S200	40	200
F40S300	40	300
F40S400	40	400
F30S200	30	200
F30S300	30	300
F30S400	30	400

further analysis. Freezing was not conducted to prevent texture changes from ice crystal formation.

Integrity Index

The integrity index was determined using the method from Samard and Ryu (2019b). About 5 g of the dried sample was rehydrated in 100 mL of distilled water at 80 °C for 30 min and was immediately autoclaved using a Hanshin autoclave HS-3041VD (Incheon, Korea) at 121 °C for 15 min above 103 kPa. The sample was then dispersed with a T-25 digital ultra-turrax disperser (IKA, BW, Germany) with 100 ml of distilled water at 17,530 g for 1 min and passed through a 20-mesh sieve. Lastly, the sample was dried at 105 °C for 16 h until a constant weight was reached. Triplicate measurements were obtained from each condition. Integrity index was calculated using the equation below.

$$Integrity\ index\ (g/kg) = \frac{Dry\ sample\ weight}{Initial\ sample\ weight} * 1000$$

Water and Oil Absorption Capacity (WAC and OAC)

WAC and OAC were determined using the method outlined by Samard et al. (2019). Extrudate was dried at 105 °C for 16 h until a constant weight was reached and was ground with a mortar and pestle. About 1 g was weighed and mixed with 10 mL of canola oil or water and mixed for 1 min using a test tube shaker (IKA Vortex 1). The samples were then placed in a water bath at 30 °C for 30 min and centrifuged using a Beckman Coulter Allegra X-12R centrifuge (Indianapolis, IN, USA) for 30 min at 25 °C, 1006 g. The supernatant was decanted, and the residue was weighed. Triplicate

measurements were obtained from each condition. Water/oil absorption capacity was calculated using the equation below.

$$Water/Oil\ absorption\ capacity(g) = \frac{X3 - X2}{X1} * 100$$

where
X1: weight of initial dry sample (g)
X2: weight of tube and dry sample (g)
X3: weight of tube and sediment after centrifugation and draining (g)

Colour Measurement

Colour measurement of extrudate was conducted as per the method of Holman et al. (2018) using a Nix Pro Color Sensor™ (Nix Sensor Ltd., ON, Canada) at 45/0° measuring geometry and 14.0 mm aperture. The observer settings used were Illuminant D65 and 10° standard observer settings. Triplicate measurements of L* (lightness), a* (greenness-redness) and b* (blueness-yellowness) were recorded for each sample according to the CIELAB colour space. Hue and chroma were calculated from a* and b* using the following equations.

$$Chroma = \sqrt{a^{*2} + b^{*2}}$$

$$Hue = tan^{-1}\left[\frac{b^*}{a^*}\right]$$

Texture Profile Analysis

Texture profile analysis was analysed using the method outlined by Zahari et al. (2020). Three 2×2 cm samples with 7 mm thickness from each extrusion condition were hydrated at 80 °C for 30 min and drained for 15 min. The hydrated extrudate was subject to texture profile analysis using a Lloyd TA1 texture analyser (Largo, FL, USA) equipped with a 18-mm cylindrical probe. Samples were probed twice at a speed of 1 mms^{-1} with three measurements per sample. Parameters of hardness, cohesiveness, chewiness and springiness were determined using NexygenPlus Materials Testing software (Largo, FL, USA).

Texturization Index

Texturization index was analysed using the method outlined by Mazlan et al. (2020). Three 2×2 cm samples of extrudate from each trial were placed in a boiling water bath at 100 °C for 30 min and then cooled for 30 min at room temperature. Samples were sheared in parallel and vertical directions respective to the flow of the cooling field using a Warner–Bratzler stainless steel shear probe

(shear angle 60°, probe thickness:1.00 mm) attached to the Lloyd TA1 texture machine. Samples were sheared to 100% of its original thickness at a speed of 1 mms^{-1}. The texturization index was calculated using the equation below. Measurements were replicated three times per sample.

$$Texturisation\ index = \frac{Lengthwise\ cutting\ strength\ F(g)}{Crosswise\ cutting\ strength\ F(g)}$$

Expansion Ratio

Expansion ratio was determined using the method adapted from Mazlan et al. (2020). Triplicate measurements of width and height of extrudate were measured from each sample with a digital calliper. These measurements were used to calculate sample area, which was subsequently averaged and inputted in the equation below.

$$Expansion\ ratio = \frac{Area\ of\ extrudate\ (mm^2)}{Area\ of\ die\ (mm^2)}$$

Apparent Density

Apparent density was analysed using the method adapted from Mazlan et al. (2020). Three samples of extrudate from each condition were weighed using an analytical balance, which were subsequently averaged. The dimensions of the extrudate were subsequently measured using a digital calliper. These results were inputted into the equation below to calculate apparent density.

$$Apparent\ density\ (kg/m^3) = \frac{W}{\pi * r^2 * L}$$

where

    W = weight of extrudate (kg)
    r = radius of extrudate (m)
    L = length of the extrudate (m)

Data Analysis

Results of texture, functional and colour data were analysed by conducting two-way analysis of variance (ANOVA) and Fischer's least significance difference (LSD) post hoc test using Minitab software 19.2020.2.0 (Minitab, PA, USA) to determine whether significant differences were present between extrusion groups. The sample means were significantly different at $p \leq 0.05$. Correlation coefficients (r) were determined using Pearson's linear correlation at a significance of $p \leq 0.05$.

Results and Discussion

Visual Appearance and Colour

The appearance of meat analogues products plays a critical role toward consumer acceptance and is thus considered one of the most important product characteristics (Kim et al., 2021). At 60% FMC, samples were bright green, visibly damp with no texturization and a crumbly, gritty texture (Table 2). Contrastingly, extrudates at 50% FMC were mealy and brittle with significant texturization and expansion only with condition F50S400 (Table 2). At 40% FMC, samples were flaky and malleable and had good texturization and expansion with optimal characteristics obtained at condition F40S400 (Table 2). Parabolic flow patterns were also the largest at condition F40S400, however, were also observed in conditions F50S400, F40S200, F40S300, F30S300 and F30S400 (Table 2). Lastly, at 30% FMC, samples were brittle, hard and dark with texturization and expansion only in conditions F30S300 and F30S400 (Table 2). Despite being heavily expanded, the expansion extrudate at condition F30S400 was not homogenous, with a cavity in the centre, webbed sporadically and a dense outer layer which was very hard (Table 2). While differences in appearances were more prominently observed between FMC, changes were also observed between SRS (Table 2). While no changes between SRS were observed at 60% FMC, increasing SRS at 50% and 40% FMC resulted in a more texturized, expanded and fibrous product (Table 2). At 30% moisture, increasing SRS resulted in a more expanded and fibrous product, but also resulted in the formation of a thick outer casing (Table 2).

The CIELAB scale is a three-dimensional colour space used to measure and quantify colours. Significant differences were observed for $L*$ and $b*$ between FMC and SRS ($p < 0.05$; Table 3) and the interaction between these factors ($p < 0.05$). Significant interactions were only observed between SRS for $a*$ ($p < 0.05$) and FMC for chroma ($p < 0.05$), while no significant differences were observed between FMC or SRS for hue (Table 3). From visual observations, it was noted that increasing FMC and decreasing SRS produced a lighter product, which was reflected in significantly higher $L*$ at 60% FMC compared to lower FMC (Tables 2 and 3), which aligns with results of Zahari et al. (2020). This is reinforced by a significant positive correlation observed between $L*$ and FMC ($r = 0.69$, $p < 0.01$; Table 6). There was also significantly higher a* values in condition F30S400 indicating that it was redder than other extrudates, which aligns with visual observations of condition F30S400 possessing brownish colour notes (Tables 2 and 3). The $b*$ value was the highest at conditions F60S200, F60S300, F60S400 and F50S200 indicating stronger yellow tones in the product at these

conditions (Table 3). The results found for $b*$ align with do Carmo et al. (2021) who found increasing FMC led to more yellowness and is further supported by a significant positive correlation between $b*$ and FMC ($r = 0.71$, $p < 0.01$; Table 6). It is however important to note that $b*$ value was subsequently increased at higher screw rotation speeds with 30% FMC, which could be due to the browning of the extrudate (Table 3). Fang et al. (2014) explained that lower FMC and higher SRS increase specific mechanical energy, create higher frictional heat and increase temperature, positively influencing the Maillard reaction,

which may contribute to the darkening of the extrudate. However, other browning reactions also contribute to the darkening of the extrudate including caramelization, non-enzymatic browning, degradation of pigments and oxidation of lipids (Ma & Ryu, 2019; Zahari et al., 2020). These browning reactions would be beneficial to the HPC from a sensory perspective as they mask the otherwise inherent bright green colour and more closely resemble the colour of meat. Other authors have not reported hue and chroma values for meat analogues; however, reporting such values is necessary for accurate colour measurement.

Table 2 Visual observations (cross-sectional photographs) of extruded hempseed protein concentrate at varying feed moisture contents and screw rotation speeds

Condition	Observations	
F60S200	- No expansion - No parabolic flow patterns - Homogenous texture with no texturization - Crumbly and mealy - Very soft and easily deformed - Damp when touched - Vibrant green with light green patches and rough surface	
F60S300	- No expansion - No parabolic flow patterns - Homogenous texture with no texturization - Crumbly and mealy - Very soft and easily deformed - Damp when touched - Vibrant green with light green patches and rough surface	
F60S400	- No expansion - No parabolic flow patterns - Homogenous texture with no texturization - Crumbly and mealy - Very soft and easily deformed - Damp when touched - Vibrant green with light green patches and rough surface	
F50S200	- Slightly expanded with no large pockets of expansion - No parabolic flow patterns - Homogenous texture with no texturization - Mealy and brittle with no malleability - No wetness when touched - Dark green color with light green ripples and smooth surface	
F50S300	- Slightly expanded with no large pockets of expansion - No parabolic flow patterns - Homogenous texture with no texturization - Mealy and brittle with no malleability - No wetness when touched - Very dark green color with light green ripples smooth surface	
F50S400	- Moderately expanded with expanded sections in the center with no expansion along perimeter - Moderate parabolic flow pattern - Texturization visible in center only - No wetness when touched - Mealy and brittle with some malleability - Very dark green color with light green ripples and large ridges on surface	

Table 2 (continued)

F40S200	• Slightly expanded with no large pockets of expansion • Moderate parabolic flow pattern • Moderate texturization • Malleable texture with no mealiness and slightly flakey texture • No wetness when touched • Very dark green color with light green ripples smooth surface
F40S300	• Moderately expanded with slightly expanded sections in the center with no expansion along perimeter • Clear parabolic flow pattern • Texturization visible in center only • No wetness when touched • Malleable with no mealiness and visible flakiness • Very dark green color with light green ripples and large ridges on surface
F40S400	• Heavily expanded with only section small perimeter not expanded • Clear parabolic flow pattern • Texturization extremely visible throughout most of the sample • No wetness when touched • Malleable with no mealiness and flakiness visible • Very dark green color with light green ripples and very large ridges on surface
F30S200	• Slightly expanded with no large pockets of expansion • No parabolic flow patterns • Homogenous texture with no texturization • Very brittle and hard • No wetness when touched • Very dark green color with light green ripples smooth surface • Burning smell upon extrusion
F30S300	• Moderately expanded with slightly expanded sections in the center with no expansion along perimeter • Moderate parabolic flow pattern • Texturization visible in center only • No wetness when touched. • Extremely brittle and hard • Very dark green color with light green ripples with large ridges on surface • Burning smell upon extrusion •
F30S400	• Heavily expanded with heavily expanded center and very dense, thick outer casing • Clear parabolic flow pattern • Texturization extremely visible throughout most of the sample • No wetness when touched • Extremely brittle and hard • Very dark green/brown color with light green ripples with very large ridges on surface • Burning smell upon extrusion

Textural Characteristics

Texturization Index

Texturization index is the ratio of maximum cutting strength in the lengthwise (longitudinal) and parallel (transverse) direction of an object (Mazlan et al., 2020). The metric is an indication of fibrous structure formation after extrusion which is essential for meat-like textures and structures in meat analogues (Kim et al., 2021), and is considered a more effective method of assessing fibre formation than texture profile analysis (Palanisamy et al., 2019). If there is no texturization, the lengthwise and parallel cutting strengths are similar, resulting in a texturization index of approximately 1. However, when fibrous structures form, the lengthwise cutting strength increases, resulting in an increased texturization index above 1 (Osen et al., 2014).

Significant differences were observed in texturization index between FMC ($p < 0.05$) but not between SRS with significantly higher texturization indexes observed at 40%

Table 3 Colour measurements of extruded hempseed protein concentrate using CIELAB colour space, hue and chroma at varying feed moisture contents and screw rotation speeds

CONDITION	L*	A*	B*	CHROMA	HUE (°) NSD
F60S200	32.84 ± 0.46bC	1.22 ± 0.08A	13.75 ± 0.17cD	13.82 ± 0.69a	1.48 ± 0.05
F60S300	33.89 ± 0.61bC	0.57 ± 0.11A	13.47 ± 0.23cE	13.35 ± 0.44a	0.47 ± 1.55
F60S400	29.30 ± 0.18bD	1.82 ± 0.10A	13.24 ± 0.22bE	13.39 ± 0.27a	1.44 ± 0.06
F50S200	29.70 ± 0.19bC	1.77 ± 0.05A	11.31 ± 0.15bD	9.97 ± 0.18a	1.40 ± 0.03
F50S300	27.45 ± 0.21aC	1.44 ± 0.02A	9.95 ± 0.09aE	10.05 ± 0.88a	1.43 ± 0.02
F50S400	29.47 ± 0.26bC	1.68 ± 0.04A	9.82 ± 0.12aE	11.45 ± 0.52a	1.42 ± 0.04
F40S200	23.50 ± 0.13aC	1.25 ± 0.02A	8.24 ± 0.09aD	8.33 ± 0.87a	1.42 ± 0.02
F40S300	24.15 ± 0.28aC	0.17 ± 0.05A	7.63 ± 0.07bE	7.73 ± 0.75a	1.42 ± 0.06
F40S400	24.43 ± 0.96aC	1.40 ± 0.05A	8.90 ± 0.09aE	9.01 ± 0.95a	1.42 ± 0.04
F30S200	24.13 ± 0.15aC	0.90 ± 0.03A	6.74 ± 0.15aD	6.80 ± 1.53a	1.44 ± 0.01
F30S300	25.35 ± 0.14aC	1.45 ± 0.04A	9.79 ± 0.10aE	9.89 ± 1.03b	1.43 ± 0.02
F30S400	25.99 ± 0.29abC	2.09 ± 0.09B	11.14 ± 0.17abE	11.35 ± 0.78b	1.39 ± 0.06

All values are presented as mean ± standard deviation. Different lowercase letters indicate a significant difference ($p \leq 0.05$) between different feed moisture contents within each screw rotation speed. Refer to Table 1 for different feed moistures and screw rotation speeds used for conditions. Different uppercase letters indicate a significant difference ($p \leq 0.05$) between screw rotation speeds within each feed moisture content. NSD indicates that no significant difference was observed between screw rotation speed nor feed moisture

FMC than 50% and 60% (Table 4). These results contradict findings by Maung et al. (2021) who found that the texturization index was significantly affected by SRS but not FMC. This discrepancy may not only be due to inherent differences between raw materials, but also due to the wide range of FMC tested in this study as Maung et al. (2021) only tested narrow FMC ranges (55–65%). Extrudate at 60% FMC had a low texturization index due to similar parallel and longitudinal cutting strengths which was reflected in visual observations with no fibrous structure formation (Tables 2 and 4). As FMC

decreased, texturization index increased, which aligns with the significant negative correlation found between texturization index and FMC ($r = -0.77$; $p < 0.01$; Table 6). Beniwal et al. (2021) explained that above a critical FMC, there is a reduction in friction between protein molecules, reducing viscous dissipation which results in incomplete denaturation, lower specific mechanical energy, less fibre formation and a lower texturization index. Increasing FMC also reduces feed protein content, decreasing the density of reactive functional groups, which otherwise interact and form chemical bonds for the fibrous structure (Beniwal et al., 2021). This may

Table 4 Texturization index and texture profile analysis measuring hardness, springiness, chewiness and cohesiveness of extruded hempseed protein concentrate at varying feed moisture contents and screw rotation speeds

Condition	Texturization index	Hardness (g/cm^2)	Springiness (%)	Chewiness (g)	Cohesiveness (%)
F60S200	1.00 ± 0.09a	115.03 ± 8.33aD	14.76 ± 1.15aD	399.92 ± 10.13aD	16.35 ± 4.85aD
F60S300	1.02 ± 0.10a	119.65 ± 15.12aD	14.04 ± 0.65aD	394.83 ± 5.92aD	15.27 ± 2.56aD
F60S400	1.01 ± 0.04a	118.87 ± 17.20aD	13.61 ± 1.05aD	383.21 ± 6.92aD	19.33 ± 2.77aD
F50S200	1.08 ± 0.05a	519.06 ± 15.71bD	30.74 ± 1.30bD	906.86 ± 6.88bD	37.39 ± 1.85bD
F50S300	1.11 ± 0.04a	527.41 ± 7.37bD	32.69 ± 0.87bD	1268.58 ± 14.62bE	38.07 ± 1.61bD
F50S400	1.16 ± 0.14a	525.69 ± 3.73bD	40.15 ± 0.48bE	1362.97 ± 12.62bF	43.58 ± 3.77bD
F40S200	1.13 ± 0.45b	914.53 ± 11.00cD	39.35 ± 0.53cD	1487.04 ± 11.23cD	52.20 ± 4.82cD
F40S300	1.49 ± 0.16b	1322.41 ± 20.67cE	49.43 ± 1.10cE	2477.76 ± 14.32cE	52.69 ± 0.49cD
F40S400	1.68 ± 0.06b	1211.74 ± 15.26cF	57.92 ± 1.44cF	2955.20 ± 20.06cF	59.56 ± 3.25cE
F30S200	TMTC	TMTC	TMTC	TMTC	TMTC
F30S300	TMTC	TMTC	TMTC	TMTC	TMTC
F30S400	TMTC	TMTC	TMTC	TMTC	TMTC

All values are presented as mean ± standard deviation. Different lowercase letters indicate a significant difference ($p \leq 0.05$) between different feed moisture contents within each screw rotation speed. Refer to Table 1 for different feed moistures and screw rotation speeds used for conditions. Different uppercase letters indicate a significant difference ($p \leq 0.05$) between screw rotation speeds within each feed moisture content. TMTC indicates that texturization index could not be measured as it exceeded the force capacity of 1000 N of the texture analyser

account for the lower texturization index observed at 60% FMC. The texturization index of 40% FMC samples was found to be significantly higher than 50% and 60% treatments, with the highest texturization index recorded for condition F40S400 (Table 4). At 30% FMC, the extrudate was very hard and possessed a thick casing at condition F30S400 and thus could not be measured as it exceeded the force capacity of 1000 N of the texture analyser (Table 4). However, visual observations indicated that fibrous structures were present in conditions F30S300 and F30S400 (Table 4). The texturization indexes observed at conditions F40S300 and F40S400 were similar to texturization indexes identified for wheat gluten and soy high moisture meat analogues, cooked chicken breast and drumstick meat (Mazlan et al., 2020; Table 4). This indicates that under certain conditions, extruded HPC can produce a product with texturization akin to meat counterparts.

Although there were differences in texturization index between screw rotation speeds, these changes were not significant ($p > 0.05$) among extruded samples (Table 4). Maung et al. (2021) declared that increasing SRS increases specific mechanical energy, which in turn reduces texturization and texturization index. Contrastingly, Zhang et al. (2019) stated that increasing SRS to a certain degree increases texturization due to increased mixing and shear and friction; however past a critical SRS, it leads to a weaker structure due to degradation of the protein structure. The results indicate that degradation of protein did not occur as the texturization index was found to increase with higher SRS (Table 4).

Textural Profile Analysis

Texture profile analysis (TPA) is an important test as it instrumentally assesses the textural characteristics of food products (Brishti et al., 2021). Four parameters were tested in TPA, namely cohesiveness, springiness, hardness and chewiness. Cohesiveness quantifies the internal resistance of food structure while springiness measures elasticity by determining the extent of recovery between the first and second compression (Ma & Ryu, 2019). Hardness is the force for a predetermined deformation, while chewiness is the energy needed to chew a solid food until it is ready for swallowing (Ma & Ryu, 2019). Significant differences were seen for all TPA parameters between FMC and SRS ($p < 0.05$; Table 4) and the interaction between FMC and SRS ($p < 0.05$) for all parameters except cohesiveness. All TPA parameters increased with decreasing FMC and increasing SRS, yet data could not be obtained for extrudate made at 30% FMC as it exceeded the force capacity of 1000 N of the texture analyser (Table 4). While there are no ideal values for TPA, it is useful to compare extrusion conditions and identify effects on texture.

The results obtained are unlike those of Maung et al. (2021) who tested a blend of soy protein isolate, wheat gluten and corn starch. The authors found that FMC and SRS significantly affected chewiness and hardness, but not springiness and cohesiveness (Maung et al., 2021). They found that increasing SRS and FMC sharply decreased hardness and chewiness, which also contradicts findings that increasing SRS led to higher TPA parameters (Table 4). Maung et al. (2021) explained that higher SRS and FMC leads to lower viscosity and elasticity inside the barrel resulting in a softer textured product. Specifically for SRS, increasing SRS increases shearing, friction and specific mechanical energy however, higher SRS can cause further degradation of the native protein structure, particularly secondary protein structures, reducing viscosity, specific mechanical energy and polymerization (Beniwal et al., 2021). The results indicated that the SRS was not high enough to cause degradation of protein and a softer product; however, this may have occurred for the products of Maung et al. (2021). Regarding the effect of FMC, increasing FMC reduces the degree of protein denaturation, protein interaction and cross linking, which ultimately leads to a softer texture (Chen et al., 2010). Ferawati et al. (2021) noted this as the reason for decreased hardness and chewiness observed at higher FMC. This may also account for the trends observed and the strong negative correlation between hardness, cohesiveness, springiness and chewiness and FMC ($r = -0.97$, $r = -0.96$, $r = -0.94$ and $r = -0.90$ respectively, $p < 0.01$; Table 6). While such mechanisms have been proposed, the exact molecular relationship between extrusion parameters and softer product texture is still to be explored (Maung et al., 2021).

Functional Characteristics

Expansion Index and Apparent Density

The expansion index is a direct measure of expansion and is based on the ratio of the extrudate diameter to the die diameter. Expansion occurs when the superheated molten mass in a high-pressure environment exits from a restricted die to a normal atmosphere (Brishti et al., 2021). The drastic drop in pressure and escape of steam promotes puffing of starch granules which results in an expanded product (Zhang et al., 2019). As expansion occurs, density is lowered. Significant differences were observed in apparent density between samples of different SRS ($p < 0.05$; Table 5), while significant differences in expansion index were observed between SRS, FMC ($p < 0.05$; Table 5) and the interaction between SRS and FMC ($p < 0.05$). As observed in Table 5, decreasing FMC and increasing SRS tended to increase expansion and decrease density.

Table 5 Density, expansion index, water absorption capacity, oil absorption capacity and integrity index of extruded hempseed protein concentrate at varying feed moisture contents and screw rotation speeds

Condition	Density (g/ cm^3)	Expansion index	Oil absorption capacity (g/g)	Water absorption capacity (g/g)	Integrity index
F60S200	1.09±0.03A	1.00±0.03aC	52.03±2.60aE	116.13±3.11aE	0±0aE
F60S300	1.11±0.03A	1.00±0.01aC	55.04±2.08aE	136.98±3.86aF	0±0aE
F60S400	1.18±0.03A	1.00±0.02aD	54.39±0.77aE	144.94±2.45aG	0±0aE
F50S200	1.20±0.04B	1.04±0.02bC	51.57±2.93aE	118.47±3.36aE	10.00±1.54bE
F50S300	1.27±0.05B	1.04±0.01bC	54.11±2.43aE	125.13±3.16bF	12.07±1.41bF
F50S400	0.89±0.01A	1.27±0.01bD	63.88±2.27bF	141.00±2.72aG	10.69±1.64bEF
F40S200	1.24±0.19A	1.04±0.03bC	53.72±2.36abE	175.17±1.06bE	33.01±0.82cE
F40S300	1.30±0.35A	1.10±0.02bC	56.92±3.24aE	198.89±4.45cF	45.44±0.67cF
F40S400	1.01±0.01A	1.17±0.03bD	73.47±3.01cF	225.09±3.75bG	57.90±0.81cG
F30S200	1.34±0.09A	1.02±0.03bC	56.36±1.83aE	200.33±5.24cE	51.14±0.81dE
F30S300	1.26±0.08A	1.062±0.01bC	74.74±4.13bF	217.06±4.24dF	57.52±1.59dF
F30S400	0.75±0.01A	1.33±0.03bD	86.99±2.55cG	297.98±2.93cG	63.87±0.32dG

All values are presented as mean±standard deviation. Different lowercase letters indicate a significant difference ($p \leq 0.05$) between different feed moisture contents within each screw rotation speed. Refer to Table 1 for different feed moistures and screw rotation speeds used for conditions. Different uppercase letters indicate a significant difference ($p \leq 0.05$) between screw rotation speeds within each feed moisture content

The generation of expansion requires sufficient FMC to ensure full hydration of the melt, which enables polymerization of protein molecules required to retain an expanded shape upon exiting the die (Zhang et al., 2019). Day and Swanson (2013) stated that at reduced FMC, the increase in melt viscosity increases entrapment of bubbles and creates high pressure at the die favouring bubble growth. This may account for the increased expansion at 30% and 40% FMC samples (Table 5). However, excessive FMC reduces viscous dissipation and moisture vaporization at the die, reducing expansion and increasing density (Brishti et al., 2021), which may account for the low expansion and high density observed at 60% FMC (Table 5). This is also supported by Alam et al. (2016) who stated that increasing FMC decreases

expansion and increases the bulk density of extrudate, which was mirrored in the significant negative correlation between expansion index and FMC ($r = -0.48$, $p < 0.05$; Table 6). Contrastingly, a higher SRS increased shearing, thermal energy and barrel pressure resulting in more air cells forming upon exiting the die (Mazlan et al., 2020). This resulted in a more expanded product with a higher expansion index and a lower density. This is supported by the significant positive correlation between expansion index and SRS ($r = 0.58$, $p < 0.01$; Table 6) and the significant negative correlation between density and SRS ($r = -0.56$, $p < 0.01$; Table 6). Density was the lowest for extrudates which had the most expansion, with a correlation between density and expansion of $r = -0.58$ ($p < 0.01$) (Tables 5 and 6). This aligns with the

Table 6 Correlation matrix of extrusion parameters and final product functional, texture and colour characteristics

	Moisture	SRS	L	a*	b*	TI	Density	EI	WAC	OAC	II	Hardness	Springiness	Chewiness	Cohesiveness
Moisture	1														
SRS	0.05	1													
L	0.69**	-0.02	1												
a*	-0.04	0.22	-0.24	1											
b*	0.71**	0.08	0.73**	0.18	1										
TI	-0.77**	0.08	-0.56**	0.20	-0.78**	1									
Density	-0.01	-0.56**	-0.02	-0.32	-0.38	0.26	1								
EI	-0.48*	0.58**	-0.41	0.63**	-0.30	0.44	-0.58**	1							
WAC	-0.78**	0.40**	-0.56**	0.07	-0.45**	0.79**	-0.33	0.56**	1						
OAC	-0.59**	0.56**	-0.26*	0.17	-0.14	0.59**	-0.57**	0.72**	0.79**	1					
II	-0.95**	0.16	-0.67**	0.10	-0.61**	0.89**	-0.08	0.49**	0.92**	0.75**	1				
Hardness	-0.97**	0.10	-0.79**	0.08	-0.85**	0.91**	0.14	0.48**	0.84**	0.66**	0.96**	1			
Springiness	-0.94**	0.24	-0.73**	0.19	-0.80**	0.84**	-0.08	0.68**	0.78**	0.78**	0.92**	0.94**	1		
Chewiness	-0.90**	0.31	-0.72**	0.13	-0.76**	0.95**	-0.02	0.60**	0.87**	0.82**	0.96**	0.96**	0.97**	1	
Cohesiveness	-0.96**	0.11	-0.78**	0.19	-0.85**	0.75**	0.06	0.61**	0.72**	0.68**	0.89**	0.93**	0.96**	0.91**	1

All values are presented as the Pearson coefficient (r). Asterisks indicate significance with one asterisk (*) indicating significance at p≤0.05 and two asterisks (**) indicating significance at p<0.01. TI: Texturization index, EI: Expansion index, WAC: Water absorption capacity, OAC: Oil absorption capacity, II: Integrity index.

results of Ma and Ryu (2019) who found an inverse relationship between expansion index and density.

Expansion is not desirable in high moisture extrusion as this detracts from meat-like textures and is often hampered by temperatures below 100 °C in the cooling die which reduces viscous dissipation of energy during gelation and restructuring of protein (Kim et al., 2021). Contrastingly for low moisture extrusion, exothermic expansion is desirable and required to produce an expanded, sponge-like texture (Zhang et al., 2019).

Water and Oil Binding Properties

Water and oil binding properties were assessed by measuring water absorption capacity (WAC) and oil absorption capacity (OAC) which are defined as the amount of water or oil that can be absorbed per gramme of protein material (Brishti et al., 2017). The OAC and WAC of proteins are essential for product quality in terms of juiciness, texture, mouthfeel, reducing moisture loss, maintaining freshness and retaining flavour (Shen et al., 2021; Vatansever et al., 2020). Significant differences were observed for OAC and WAC between FMC and SRS ($p < 0.05$; Table 5) and the interaction between these factors ($p < 0.05$). The trend observed was that lower FMC and higher SRS resulted in higher values for WAC and OAC (Table 5). This aligns with negative correlation between OAC and WAC and FMC ($r = 0.59$, $p < 0.01$; $r = -0.78$, $p < 0.01$; Table 6) and between WAC, OAC and SRS ($r = 0.56$, $p < 0.01$; Table 6).

At high FMC and low SRS, there is incomplete denaturation of protein due to decreased viscous dissipation (Beniwal et al., 2021; Chen et al., 2010). However, as FMC decreases and SRS increases, friction and shear stress increase, increasing protein denaturation (Beniwal et al., 2021; do Carmo et al., 2021). As denaturation of native proteins occurs, buried hydrophilic groups become exposed, increasing water binding and reducing oil binding compared to raw materials (Osen et al., 2014). While this explanation may explain the increased WAC, it does not explain the higher OAC at lower FMC and increased SRS contents, as increased surface hydrophilicity would reduce oil binding capacity. The increased OAC could be due to the inherent oil binding properties of hempseed protein when extruded, although there have been no studies assessing the behaviour of extruded hempseed protein. Water and oil binding of proteins is also affected by many intrinsic and extrinsic factors including protein concentration, amino acid profile, conformation, pH, hydrophobicity, ionic strength and temperature (Wang & Xiong, 2019).

While the WAC and OAC values for extruded hempseed protein have not been reported, the WAC and OAC observed were lower than other protein sources studied by Brishti et al. (2021), Samard et al. (2019) and Tehrani et al.

(2017). While the desirable range for these parameters is based on its end use, a high value is often desirable for most meat analogue application (Vatansever et al., 2020). Samard et al. (2019) stated that a high WAC would make the TVP suitable in viscous foods which require high water retention including gravies and soups, while a higher OAC would make the TVP suitable for use as a meat extender in meat emulsions and oil-based emulsions. The lower WAC observed for the HPC is possibly due to the relatively lower protein content and higher lipid content of the HPC ("Materials and Sample Preparation"). As observed by Teh et al. (2014), higher oil content in the raw materials can reduce the OAC. This is further supported by Galves et al. (2019) who found that defatting HPC increased OAC, attributed to more hydrophobic binding sites as lipids were removed after defatting. The results could also be influenced by aggregation of hempseed protein, specifically the edestin fraction, which when aggregated buries hydrophilic groups and reduces water binding (Tang et al., 2006).

Integrity Index

The integrity index is a measure of the residue after the TVP is hydrated, pressurized, homogenized and dried and ultimately affects the quality and yield of TVP (Samard & Ryu, 2019b). A high integrity index signifies texturization between protein molecules which results in lower solid loss and enhanced product quality (Brishti et al., 2021). Significant differences were observed between the integrity index and FMC and SRS ($p < 0.05$; Table 5) and the interaction between these factors ($p < 0.05$). The trend observed was that decreasing FMC and increasing SRS increased the integrity index (Table 5), which is supported by a strong significant correlation between FMC and integrity index ($r = -0.95$, $p < 0.01$; Table 6). This aligns with other authors' observations that increasing FMC reduces the integrity of the product (Chen et al., 2010; Palanisamy et al., 2019). Samard and Ryu (2019b) further stated that the formation of the fibrous structures produces a high-integrity product, while a product with low texturization would have low integrity. This is supported by a strong positive correlation between texturization index and integrity index ($r = 0.89$, $p < 0.01$; Table 6). Such strong texturized structures can withstand high pressures and temperatures during autoclaving and homogenization better than weaker texturized products (Samard & Ryu, 2019b). Brishti et al. (2021) suggested that high cohesiveness is associated with high integrity as it minimizes solid loss. This is supported by the present results which indicate a strong correlation between cohesiveness and integrity index ($r = 0.89$, $p < 0.01$; Table 6). The integrity index values reported in the literature vary greatly with TVP made from isolated soy protein having an integrity index between 6.02 and 13.52% while TVP made from vital wheat gluten

and isolated soy protein ranging between 73.4 and 91.1% (Samard & Ryu, 2019a). In addition to differences in texturization and cohesiveness, this high variation may be due to differences between raw materials (Brishti et al., 2021).

Correlation Between Extrusion Parameters and Final Product Characteristics

As seen from the correlation matrix, there were significant correlations ($p < 0.05$) between FMC and all final product characteristics except a* value and density (Table 6). Contrastingly, significant correlations ($p < 0.05$) for SRS were only seen for expansion index, density, WAC and OAC (Table 6). Significant correlations ($p < 0.05$) were seen between WAC, OAC, expansion index, TPA parameters, and integrity index all of which were negatively correlated with FMC (Table 6). Thus, decreasing FMC tended to increase all functional characteristics except density and TPA parameters. This aligns with Samard et al. (2019) who reported significant correlations ($p < 0.05$) between springiness, hardness and integrity index. Correlations between other final product characteristics were not found in the literature. The correlations identified in this study would assist in understanding the effect of FMC and SRS on extrudate product characteristics and the relationship between such characteristics.

Conclusions

In extrusion of hempseed protein concentrate, lower FMC and SRS positively influenced texturization index, expansion index, WAC, OAC, integrity index and texture profile characteristics, but negatively influenced density, *L** and *b** values of the extrudates. Despite that extrudate at 30% FMC and 400 rpm possessed the highest WAC, OAC, texturization index and integrity index, it also possessed immeasurably high TPA parameters and undesirable structural characteristics. Contrastingly, at 60% FMC, no texturization occurred regardless of SRS and produced undesirable textural, functional and appearance characteristics. Thus, extrusion at 40% FMC and 400 rpm SRS produced the optimal overall characteristics and would thus be most suitable for use in industry as an alternative to traditional TVP in meat analogues to add value to the hempseed industry.

Author Contribution Amrut Rajendra: writing—original draft, conceptualization, methodology, formal analysis, investigation, data curation, software, visualization. Robyn Warner: supervision, writing—review, editing. Minh, Ha: supervision, writing—review, editing. Danyang Ying: supervision, writing—review, editing, investigation. Zhongxiang Fang: supervision, conceptualization, resources, project administration, writing—review, editing, funding acquisition.

Declarations

References

Alam, M. S., Kaur, J., Khaira, H., & Gupta, K. (2016). Extrusion and extruded products: Changes in quality attributes as affected by extrusion process parameters: A review. *Critical Reviews in Food Science and Nutrition, 56*(3), 445–473. https://doi.org/10.1080/10408398.2013.779568

Beniwal, A. S., Singh, J., Kaur, L., Hardacre, A., & Singh, H. (2021). Meat analogs: Protein restructuring during thermomechanical processing. *Comprehensive Reviews in Food Science and Food Safety, 20*(2), 1221–1249. https://doi.org/10.1111/1541-4337.12721

Brishti, F. H., Zarei, M., Muhammad, K., Ismail-Fitry, M. R., Shukri, R., & Saari, N. (2017). Evaluation of the functional properties of mung bean protein isolate for development of textured vegetable protein. *International Food Research Journal, 24*, 1595–1605.

Brishti, F. H., Chay, S. Y., Muhammad, K., Ismail-Fitry, M. R., Zarei, M., & Saari, N. (2021). Texturized mung bean protein as a sustainable food source: Effects of extrusion on its physical, textural and protein quality. *Innovative Food Science & Emerging Technologies, 67*, 102591. https://doi.org/10.1016/j.ifset.2020.102591

Chen, F. L., Wei, Y. M., Zhang, B., & Ojokoh, A. O. (2010). System parameters and product properties response of soybean protein extruded at wide moisture range. *Journal of Food Engineering, 96*(2), 208–213. https://doi.org/10.1016/j.jfoodeng.2009.07.014

Curtain, F., & Grafenauer, S. (2019). Plant-based meat substitutes in the flexitarian age: An audit of products on supermarket shelves. *Nutrients, 11*(11), 2603. https://doi.org/10.3390/nu11112603

Day, L., & Swanson, B. G. (2013). Functionality of protein-fortified extrudates. *Comprehensive Reviews in Food Science and Food Safety, 12*(5), 546–564. https://doi.org/10.1111/1541-4337.12023

De Angelis, D., Kaleda, A., Pasqualone, A., Vaikma, H., Tamm, M., Tammik, M. L., Squeo, G., & Summo, C. (2020). Physicochemical and sensorial evaluation of meat analogues produced from dry-fractionated pea and oat proteins. *Foods, 9*(12), 1754. https://doi.org/10.3390/foods9121754

Dekkers, B. L., Boom, R. M., & van der Goot, A. J. (2018). Structuring processes for meat analogues. *Trends in Food Science & Technology, 81*, 25–36. https://doi.org/10.1016/j.tifs.2018.08.011

do Carmo, C. S., Knutsen, S. H., Malizia, G., Dessev, T., Geny, A., Zobel, H., Myhrer, K.S., Varela, P., & Sahlstrøm, S. (2021). Meat analogues from a faba bean concentrate can be generated by high moisture extrusion. *Future Foods, 3*, 100014. https://doi.org/10.1016/j.fufo.2021.100014

Fang, Y., Zhang, B., & Wei, Y. (2014). Effects of the specific mechanical energy on the physicochemical properties of texturized soy protein during high-moisture extrusion cooking. *Journal of Food Engineering, 121*, 32–38. https://doi.org/10.1016/j.jfoodeng.2013.08.002

Ferawati, F., Zahari, I., Barman, M., Hefni, M., Ahlström, C., Witthöft, C., & Östbring, K. (2021). High-moisture meat analogues produced from yellow pea and faba bean protein isolates/concentrate: Effect of raw material composition and extrusion parameters on texture properties. *Foods, 10*(4), 843. https://doi.org/10.3390/foods10040843

Galves, C., Stone, A. K., Szarko, J., Liu, S., Shafer, K., Hargreaves, J., Siarkowski, M., & Nickerson, M. T. (2019). Effect of pH and defatting on the functional attributes of safflower, sunflower, canola, and hemp protein concentrates. *Cereal Chemistry, 96*, 1036–1047.

Godfray, H. C. J., Aveyard, P., Garnett, T., Hall, J. W., Key, T. J., Lorimer, J., Pierrehumbert, R. T., Scarborough, P., Springmann, M., & Jebb, S. A. (2018). Meat consumption, health, and the environment. *Science, 361*(6399), eaam5324.

Holman, B. W., Collins, D., Kilgannon, A. K., & Hopkins, D. L. (2018). The effect of technical replicate (repeats) on Nix Pro Color Sensor™ measurement precision for meat: A case-study on aged beef color stability. *Meat Science, 135*, 42–45. https://doi.org/10.1016/j.meatsci.2017.09.001

Kim, T., Riaz, M. N., Awika, J., & Teferra, T. F. (2021). The effect of cooling and rehydration methods in high moisture meat analogs with pulse proteins-peas, lentils, and faba beans. *Journal of Food Science, 86*(4), 1322–1334. https://doi.org/10.1111/1750-3841.15660

Lawrence, S., & King, T. (2019). *Meat the alternative: Australia's $3 billion opportunity*. Food Frontier.

Ma, X., & Ryu, G. (2019). Effects of green tea contents on the quality and antioxidant properties of textured vegetable protein by extrusion-cooking. *Food Science and Biotechnology, 28*(1), 67–74. https://doi.org/10.1007/s10068-018-0437-7

Maung, T. T., Gu B. Y., & Ryu, G. H. (2021). Influence of extrusion process parameters on specific mechanical energy and physical properties of high-moisture meat analog. *International Journal of Food Engineering, 17*(2), 149–157. https://doi.org/10.1515/ijfe-2020-0042

Mazlan, M. M., Talib, R. A., Chin, N. L., Shukri, R., Taip, F. S., Mohd Nor, M. Z., & Abdullah, N. (2020). Physical and microstructure properties of oyster mushroom-soy protein meat analog via single-screw extrusion. *Foods, 9*(8), 1023. https://doi.org/10.3390/foods9081023

Osen, R., Toelstede, S., Wild, F., Eisner, P., & Schweiggert-Weisz, U. (2014). High moisture extrusion cooking of pea protein isolates: Raw material characteristics, extruder responses, and texture properties. *Journal of Food Engineering, 127*, 67–74. https://doi.org/10.1016/j.jfoodeng.2013.11.023

Palanisamy, M., Franke, K., Berger, R. G., Heinz, V., & Töpfl, S. (2019). High moisture extrusion of lupin protein: Influence of extrusion parameters on extruder responses and product properties. *Journal of the Science of Food and Agriculture, 99*(5), 2175–2185. https://doi.org/10.1002/jsfa.9410

Pihlanto, A., Nurmi, M., & Mäkinen, S. (2020). Hempseed protein: Processing and functional properties. In G. Crini & E. Lichtfouse (Eds.), *Sustainable Agriculture Reviews* (Vol. 42, pp. 223–237). Springer.

Plattner, B. (2020). Extrusion techniques for meat analogues. *Cereal Foods World*, *65*(4). https://doi.org/10.1094/CFW-65-4-0043

Riaz, M. N. (2011). Texturized vegetable proteins. In G. O. Phillips & P. A. Williams (Eds.), *Handbook of Food Proteins* (pp. 395–418). Woodhead Publishing.

Richi, E. B., Baumer, B., Conrad, B., Darioli, R., Schmid, Alexandra, & Keller, Ulrich. (2015). Health Risks Associated with Meat Consumption: A Review of Epidemiological Studies. *International Journal for Vitamin and Nutrition Research, 85*(1–2), 70–78. https://doi.org/10.1024/0300-9831/a000224

Samard, S., & Ryu, G. H. (2019a). A comparison of physicochemical characteristics, texture, and structure of meat analogue and meats. *Journal of the Science of Food and Agriculture, 99*(6), 2708–2715. https://doi.org/10.1002/jsfa.9438

Samard, S., Gu, B. Y., & Ryu, G. H. (2019). Effects of extrusion types, screw speed and addition of wheat gluten on physicochemical characteristics and cooking stability of meat analogues. *Journal of the Science of Food and Agriculture, 99*(11), 4922–4931. https://doi.org/10.1002/jsfa.9722

Samard, S., & Ryu, G. H. (2019b). Physicochemical and functional characteristics of plant protein-based meat analogs. *Journal of Food Processing and Preservation, 43*(10), e14123. https://doi.org/10.1111/jfpp.14123

Shen, P., Gao, Z., Fang, B., Rao, J., & Chen, B. (2021). Ferreting out the secrets of industrial hemp protein as emerging functional food ingredients. *Trends in Food Science & Technology, 112*, 1–15. https://doi.org/10.1016/j.tifs.2021.03.022

Sun, C., Ge, J., He, J., Gan, R., & Fang, Y. (2020). Processing, quality, safety, and acceptance of meat analogue products. *Engineering, 7*(5), 674–678. https://doi.org/10.1016/j.eng.2020.10.011

Tang, C. H., Ten, Z., Wang, X. S., & Yang, X. Q. (2006). Physicochemical and functional properties of hemp (Cannabis sativa L.) protein isolate. *Journal of Agricultural and Food Chemistry*, *54*(23), 8945–8950. https://doi.org/10.1021/jf0619176

Teh, S.-S., Bekhit, A. E.-D., Carne, A., & Birch, J. (2014). Effect of thedefatting process, acid and alkali extraction on the physicochemical andfunctional properties of hemp, flax and canola seed cake protein isolates. *Journal of Food Measurement and Characterization*, *8*(2), 92–104.

Tehrani, M. M., Ehtiati, A., & Azghandi, S. S. (2017). Application of genetic algorithm to optimize extrusion condition for soy-based meat analogue texturization. *Journal of Food Science and Technology, 54*(5), 1119–1125. https://doi.org/10.1007/s13197-017-2524-9

Thrane, M., Paulsen, P. V., Orcutt, M. W., & Krieger, T. M. (2017). Soy protein: Impacts, production, and applications. In S. R. Nadathur, J. P. D Wanasundara & L. Scanlin (Eds.), *Sustainable Protein Sources* (pp. 23–45). Academic Press. https://doi.org/10.1016/B978-0-12-802778-3.00002-0

Vatansever, S., Tulbek, M. C., & Riaz, M. N. (2020). Low-and high-moisture extrusion of pulse proteins as plant-based meat ingredients: A review. *Proteins, 10*, 12–14. https://doi.org/10.1094/CFW-65-4-0038

Wang, Q., & Xiong, Y. L. (2019). Processing, nutrition, and functionality of hempseed protein: A review. *Comprehensive Reviews in Food Science and Food Safety, 18*(4), 936–952. https://doi.org/10.1111/1541-4337.12450

Webb, D., Plattner, B. J., Donald, E., Funk, D., Plattner, B. S., & Alavi, S. (2020). Role of chickpea flour in texturization of extruded pea protein. *Journal of Food Science, 85*(12), 4180–4187. https://doi.org/10.1111/1750-3841.15531

Zahari, I., Ferawati, F., Helstad, A., Ahlström, C., Östbring, K., Rayner, M., & Purhagen, J. K. (2020). Development of high-moisture meat analogues with hemp and soy protein using extrusion cooking. *Foods, 9*(6), 772. https://doi.org/10.3390/foods9060772

Zhang, J., Liu, L., Liu, H., Yoon, A., Rizvi, S. S., & Wang, Q. (2019). Changes in conformation and quality of vegetable protein during texturization process by extrusion. *Critical Reviews in Food

Science and Nutrition, 59(20), 3267–3280. https://doi.org/10.1080/10408398.2018.1487383

Publisher's Note Springer Nature remains neutral with regard to jurisdictional claims in published maps and institutional affiliations.